Tightly Coupled In Vivo Studies to Inform an In Silico Model of Acetaminophen Toxicity in Mice (year 1)

INDIANA UNIVERSITY

James Sluka, Xiao Fu, Sherry Clendenon , Victoria Sluka, James Glazier, Jennifer Ryan, Kenneth Dunn, Zemin Wang, Xilin Li, and James Klaunig

Indiana University, Bloomington and Indianapolis, Indiana

Introduction

Acetaminophen (*APAP*) overdose is the most common cause of liver failure in the western world. APAP induced liver injury was first reported over forty years ago, yet how and why APAP induced liver injury progresses to liver failure in some individuals but not in others is still not fully understood. In silico modeling offers the opportunity to better understand how liver toxicity occurs and progresses to liver failure while simultaneously reducing the numbers of animals that must be used to gain this understanding.

Pharmacological and toxicological processes occur across a wide range of spatial and temporal scales and include multiple organ systems. A *Systems Biology* in silico toxicological model must include submodels that cover the multiple scales and the multiple tissues relevant to human medicine and toxicology. We will develop a liver centered mechanism based multiscale in silico simulation framework for xenobiotic toxicity and metabolism that incorporates three key biological scales:

1.Physiologically Based Pharmacokinetic (PBPK) whole body scale
2.Tissue level and multicellular scale
3.Subcellular signaling and metabolic pathways scales

Our approach to developing the multi-scale model includes tight coupling between wet lab experiments and model building, verification and validation. Experimental outputs from all sets of experiments can be used as correlated inputs and validations for the simulations.

Preclinical Histopathology (Klaunig, Wang, Li): Drug metabolites and serum markers of liver function. Level and distribution of liver damage assessed by standard pathology.

Quantitative Intravital Imaging (Dunn, Ryan): Dynamic processes - blood flow within the liver at the sinusoid scale, trans-hepatocyte transfer kinetics, reactive oxygen species, cell proliferation/death, cell motility

Quantitative 3D Liver micro-morphology (Clendenon): Morphology - size of blood vessels and bile canaliculi, distribution and sizes of liver cell types, mitotic, apoptotic and necrotic index. Specific protein levels and spatial.

Model Building (Glazier, Sluka, Fu): Creation, verification and validation of the in silico model. Close interaction with the wet-lab groups in designing follow-up experiments.

Animals: Three mouse strains were chosen from the Mouse Phenome Database (http://phenome.jax.org/) based on their sensitivities to APAP: *CAST/EiJ* highly resistant, *C57BL/6J* mid-range sensitivity, *B6C3F1/J* highly sensitive. Note that all of these strains have the same genetic background.

Protocols:

TIME RESPONSE: Mice will be sampled 0,1,4,24,and 48 hrs post treatment

DOSE RESPONSE: Mice will be treated with saline only (control group), pharmacologic dose of acetaminophen (10 mg/kg BW), and higher doses of acetaminophen (100, 250, 500 mg/kg BW).

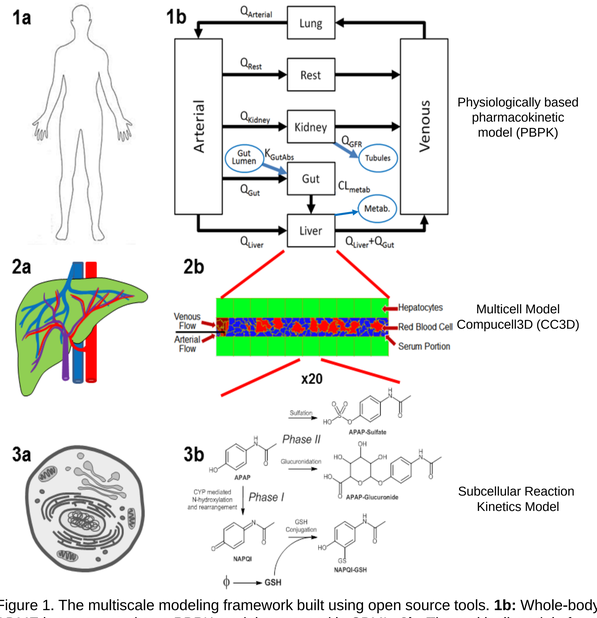

Figure 1. The multiscale modeling framework built using open source tools. **1b:** Whole-body ADME is represented as a PBPK model expressed in SBML. **2b:** The multicell model of a single simple sinusoid, lined with hepatocytes, including blood flow, is modelled in CompuCell3D. **3b:** The subcellular metabolic reactions of APAP (Phase I and Phase II) are modeled in SBML.

Histopathology: Serum markers, metabolites and tissue pathology

Initial studies established the *in vivo* APAP-induced acute liver toxicity model in the Klaunig Lab. These studies were essential to insure repeatability of the APAP induced liver toxicity model in mice and also allow for protocols that can be consistently repeated in the Klaunig and Dunn labs. In addition, livers from these initial studies were appropriately processed and provided to the Glazer Lab for their analysis. The following have been accomplished:

1. The optimization and standardization of the animal handling, treatment and exposure of the mice.
2. The proper and repeatable formulation of the drug for i.p. injection, which is critical.
3. Optimization of the euthanasia and tissue sampling procedures including blood collection, perfusion fixation of liver, tissue sampling and formalin fixation for standard histopathology examination.
4. Developed and validated analytical methods for measuring APAP and metabolites; APAP-Glth, APAP-Glc, APAP-Sul, APAP-OMe and APAP-NAC, in both serum and liver tissue samples.

A preliminary study to examine the dose-response effects of acute liver toxicity of APAP using the following experimental design has been completed. Twenty five 8-10 week old male C57BL/6 mice were treated with APAP. Mice (5/group) were assigned to five groups and administered a single dose of APAP at 10 mg/kg, 100 mg/kg, 250 mg/kg and 500 mg/kg or sterile 1X PBS (vehicle control) via i.p. injection for 24 hr. The mice had *ad libitum* access to food and water. Blood from each mouse was collected and serum samples were prepared. The serum liver enzymes, Alanine aminotransferase (*ALT*) and Aspartate aminotransferase (*AST*), were measured immediately using Infinity™ ALT and AST kits. The rest of the sample was used for metabolites analysis. The liver from one (out of 5) mouse in each group was perfusion fixed with 4% PFA and provided to the Glazier group for 3D liver structure determination. Pieces of liver from the left, median, right and caudate lobe of the remaining four mice were formalin fixed for standard histopathology examination of liver tissue damage. The rest of the liver tissue was snap frozen and stored at -80° C for future biochemical analysis including inflammatory markers, APAP and metabolites, etc. as needed.

Figure 2 shows the results of AST and ALT analysis for the dose-response study in C57BL/6J mice. A slight increase in both ALT and AST was observed after 24 hr following single i.p. injection of 10 mg/kg and 100 mg/kg APAP as compared with vehicle control. In contrast, remarkable increases in serum ALT and AST were seen following single APAP at 250 mg/kg, the increases were even more prominent at the dose of 500 mg/kg. The levels of ALT and AST corresponded to the severity of liver tissue damage, specifically hepatocyte necrosis, as seen in the standard histopathology (H&E staining) slides shown in Figure 4. Figure 3 shows typical results for tissue and serum levels of APAP and its metabolites following a single 100mg/kg i.p. dose of APAP.

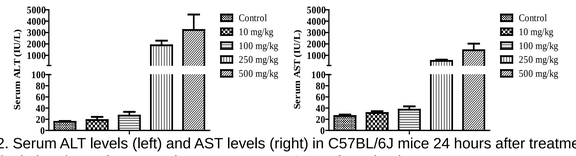

Figure 2. Serum ALT levels (left) and AST levels (right) in C57BL/6J mice 24 hours after treatment with a single i.p. dose of APAP. Values are mean ± SEM of 5 animals per group.

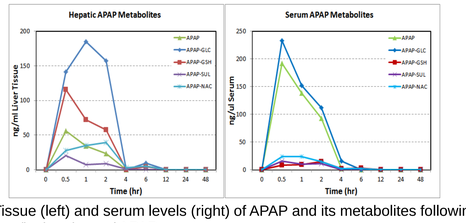

Figure 3. Tissue (left) and serum levels (right) of APAP and its metabolites following a single 100mg/kg i.p. dose of APAP

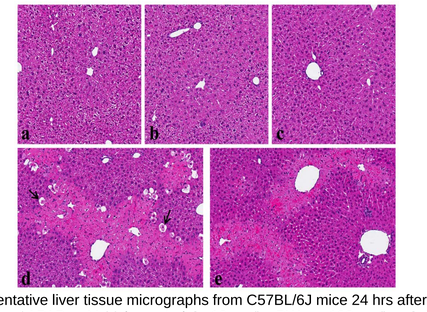

Figure 4. Representative liver tissue micrographs from C57BL/6J mice 24 hrs after treatment with single i.p. injection of APAP. **a**. Vehicle control; **b**. 10 mg/kg BW; **c**. 100 mg/kg; **d**. 250 mg/kg. Note the extensive centrilobular necrosis and ballooning degeneration of hepatocytes surrounding the necrotic area; **e**. 500 mg/kg. Showing extensive centrilobular congestion and hepatocyte necrosis. Mag. 100X.

Quantitative Intravital Microscopy

We have developed methods for high-resolution microscopy of the liver of living mice based upon methods previously developed for rat liver;

1. We developed mouse jugular cannulation for I.V. injections during surgery and on the microscope stage and comparisons showed jugular cannulations to be profoundly more reliable than tail vein cannulations. This development led to a complete protocol for surgery, probe introduction and imaging.
2. We have determined *in vivo* doses for sodium fluorescein (hepatocyte transport assay), 2 million MW dextran (microvascular perfusion and leakage assays), Hoechst 33342 (apoptosis, necrosis, white cell adhesion/rolling assays), and dihydroethidium (oxidative stress assay).
3. We have optimized imaging conditions for collagen second harmonic generation images for characterization of fibrosis. An example of an image volume collected from a living mouse following intravenous injection of 150K rhodamine dextran (labeling sinusoids red) and sodium fluorescein (labeling bile canaliculi green) is shown in Figure 5 including the second harmonic generation image of collagen (primarily in the capsule).
4. We have developed techniques to facilitate complementary biochemical and histological analyses. We developed a method of photobleaching a pattern on the imaged left lateral liver lobe to be used in histological analysis to identify regions that had been imaged by intravital microscopy. We developed a procedure for tying off a single lobe for snap freezing and paraformaldehyde perfuse-fixation of the remaining liver lobes.
5. We have conducted pilot studies of untreated mice, collecting data for 3D structure, microvascular perfusion, microvascular leakage, fluorescein transport, oxidative stress, apoptosis and necrosis.
6. We have identified a library of images collected from the liver of living rats under control and various pathological conditions, to be used to develop image processing techniques for quantitative assays of white cell adhesion/rolling, apoptosis, necrosis, microvascular flow and leakage.

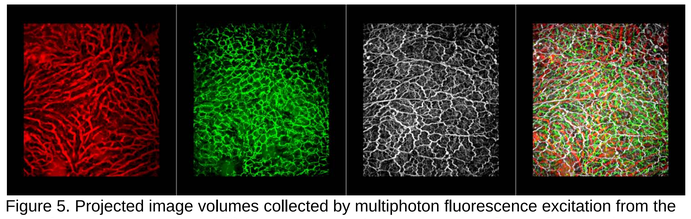

Figure 5. Projected image volumes collected by multiphoton fluorescence excitation from the liver of a living mouse. Red: 150K rhodamine dextran in sinusoids. Green: fluorescein in bile canaliculi. White: Second harmonic image of collagen. The right hand image is a composite of the three channels.

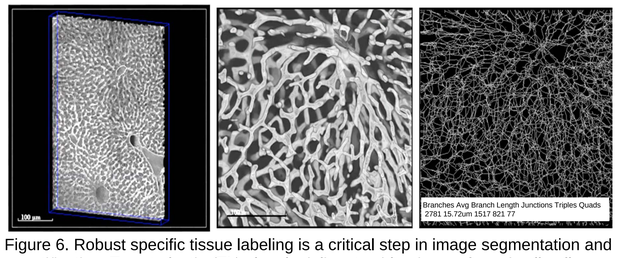

Figure 6. Robust specific tissue labeling is a critical step in image segmentation and quantification. Tomato lectin (TL) cleanly delineates blood vessels and cell-cell junctions. Left image shows a mosaic of six TL labeled 3D confocal image volumes, encompassing two central veins and two portal triads. Middle panel shows blood vessels that were hand segmented in 3D from lectin labeled images. In right panel 3D skeletonize and analysis of the 3D segmented image, for branch length and branch point analysis. Bars = 100 µm.

Acknowledgements

This research was funded by the US EPA (R835001), the NIH (GM111243 and GM077138), and Indiana University, which is gratefully acknowledged.

Quantitative 3D Liver Micro-morphology

Perfusion fixed control and APAP treated mouse livers (male C57BL/6J, 8weeks) have been obtained from both the Dunn and Klaunig groups and we have prepared hundreds of thick liver sections for microscopy.

Our initial efforts have been focused on developing robust and standardized methods for morphological staining, imaging and quantification of tissue morphology in liver. Optimization of labeling reduces the effort and increases the quality of segmentation and quantification that follow.

To obtain global 3D micro-morphology of hepatocytes, sinusoidal capillaries and bile canaliculi within a lobule we need the ability to label endothelial cells (sinusoidal capillaries and larger vessels), cell-cell junctions (to outline individual cells), bile canaliculi and ducts, and nuclei. Additionally, these labels need to be minimally affected by tissue clearing solutions so that we can obtain optical sections from 150-200 microns tissue depth. We have developed staining protocols using Tomato Lectin (*TL*) and Lens Culinaris Agglutinin (*LCA*) that allow us to use the gradient of LCA staining to define lobule zones as shown in Figure 7.

Using these staining protocols we have processed thick sections of normal mouse liver tissue. Segmentation allows us to clearly delineate the sinusoids (micro vasculature) and measure morphological quantities such as cross linking indexes (Figure 6) and sinusoid diameters across a lobule as in Figure 8.

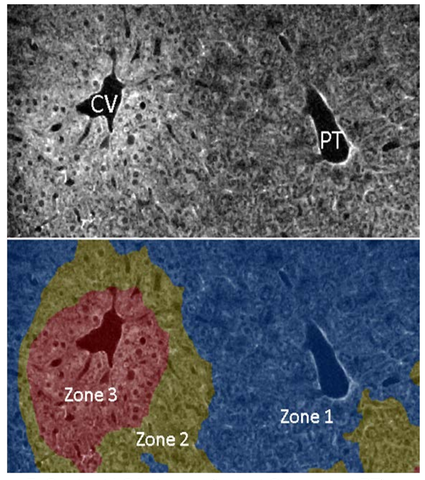

Figure 7. Gradient LCA staining (high at CV, weak at PT) can delineate lobule zonation.

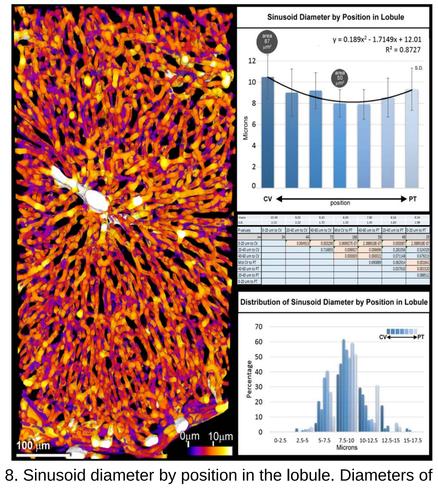

Figure 8. Sinusoid diameter by position in the lobule. Diameters of segmented sinusoids were quantified using the rolling ball algorithm, then quantified by distance from CV or PT.